Low temperature coupled oxidative/adsorptive desulfurization catalyzed by FeOOH/rGO nanocomposite

Journal of Physics: Conference Series **2830** (2024) 012014 doi:10.1088/1742-6596/2830/1/012014

Low temperature coupled oxidative/adsorptive desulfurization catalyzed by FeOOH/rGO nanocomposite

Aya M Matloob[1*], Dalia R Abd Elhafiz[1], & Deyaa Abol-Fotouh[2]

[1] Refining Department, Egyptian Petroleum Research Institute, Cairo, Egypt

[2] City of Scientific Research & Technological Applications (SRTA-City), New Burg Al-Arab, Egypt.

Aya_mtloob@epri.sci.eg

Abstract. Desulfurization of fossil fuel products has grabbed increased attention, where many research themes focus on the synthesis of novel materials with enhanced desulfurization potentialities, at a reasonable cost, and within a shorter working time. So, in this work, we synthesized ultrathin FeOOH nanorods and then anchored them over reduced graphene oxide (FeOOH/rGO nanocomposite) to act as catalyst/adsorbent system during in situ oxidative/adsorptive desulfurization of diesel fuel model. The XRD, FTIR and Raman analyses demonstrated the successful combination of the FeOOH with the rGO surface. The BET surface area of the FeOOH/rGO was enhanced by 2.2 folds compared to the parent FeOOH, with pore volume ~0.268 cc/g. TEM investigation proved the FeOOH-rGO conjugation. The catalytic processes were carried out in association with H2O2 as an oxidizing element in different conditions. FeOOH showed a high adsorption capacity of ~960 mg/g, and obeyed pseudo-second order kinetic confirming chemisorption nature, while the process Ea recorded about ~85.4 kJ/mol. On the other hand, FeOOH/rGO system achieved ultra-high adsorption capacity of ~989 mg/g with high removal efficiency (98.9%), which assumed FeOOH/rGO as a highly potential catalyst/adsorbent system for ultra desulfurization process.

1. Introduction

Fossil fuels represent a significant resource in the global energy sector; for example, in 2015, they accounted for around 86% of total worldwide energy consumption. However, burning sulfur-containing compounds in fuels adversely affects the air quality, and pose many hazards to the ecosystem [1] For instance, the permissible sulfur concentration in commercial fuels is regulated to 15 mg/g in the US and 10 mg/g in the EU [2]. Hydrodesulfurization (HDS) is a widely applied method that works well for acyclic and aliphatic S-compounds but not well enough for thiophenic compounds like dibenzothiophene (DBT) [3, 4]. Dealing with the thiophenic compounds has demanded developing novel desulfurization approaches with more facile and cheap operation conditions. Interestingly, oxidative desulfurization (ODS) associated with adsorption is counted with a great potentiality because its capability to remove sulfur compounds under ambient conditions, demanding no hydrogen consumption, and with high eco-

sustainability [5]. In oxidative desulfurization (ODS) process the DBT and other thiophenic compounds are usually transformed into the corresponding sulfoxide and sulfone species. To finally obtain a deeply desulfurized product, the sulfone species should then be removed in a second step by extraction or adsorption. Currently, developing novel and potential catalyst/oxidants has been broadly studied to enhance reaction efficiency and support the mass transfer in the interfacial region [6, 7]. Hydrogen peroxide (H_2O_2) has been assorted as an alluring oxidizing agent of S-compounds, where its desulfurization performance associated with various catalytic materials was widely investigated [8, 9].

Carbonaceous compounds (such as activated carbon or graphene) and metal oxides primarily synthesized for catalytic purposes are among the distinctive desulfurizing oxidative/adsorbents. Graphene-related materials are excellent supports owing to their exceptional physical, and electrical properties in addition to their favorable superficial chemistry, that allows for simple decoration with desired materials [10]. Since graphene derivatives have a promising future as a supportive material, it may be worthwhile to combine the advantageous properties of graphene oxide with a heterogeneous catalyst to help overcome the obstacles that oxidative processes currently face.

Herein, we studied the synthesis of iron oxide hydroxides (FeOOH), and FeOOH-rGO nanocomposite catalysts, where their performance for desulfurization at decreased temperatures was determined. The synthesized materials were featured to inspect their physical and chemical properties considered for the desulfurization process. Moreover, the desulfurization trials were accomplished at temperature (25 °C), where the catalytic activity was studied versus many factors such as the adsorbent amount, H2O2:S ratio, and reaction time. Furthermore, the reaction kinetics and thermodynamics were investigated to figure out more about the oxidation behavior and the oxidation/adsorption impact. Relying on the outputs, the relationship between the composition and adsorption capability was researched and discussed.

2. Experimental

2.1 Material synthesis

First, graphite oxide was first synthesized through enhanced Hummer`s technique, where 3 g of graphite was added to a mixture of H2SO4 (98%): 70 ml, and phosphoric acid (85%): 6.7 ml for 30 min under stirring in an ice bath. Afterward, an amount of KMnO4 proportional to the utilized graphite was added bit by bit under vigorous agitation. The blend was stirred at room temperature for 1 day. A dark green suspension which turned to a highly viscous blend emerged cluing the oxidation of the graphite and the precipitation of MnO2. To quell the reaction, 500 ml of d-H_2O was added to the mixture under stirring at reaction temperature 95 °C for 15 min, then 15 ml hydrogen peroxide was added until the yellow color emerged. The blend was allowed to stand for 12 h at least, then the clear supernatant was decanted, and the remaining precipitate was washed with hot d-H_2O. The obtained metallic grey graphene oxide (GO) precipitate was collected and dried at room temperature.

Second, ultra-sonication was used to synthesize FeOOH nanoparticles. Briefly, FeCl3.6H2O was hydrolyzed with NH4OH to adjust pH at 8. The precipitate is then gathered by centrifuge and dried overnight at 80 °C. To prepare FeOOH/rGO nanocomposite, two grams of the synthesized GO faded in 300 ml d-H2O and sonicated for 1 h. After that, 1.1 g of FeCl3.6H2O was added into the suspension and ultrasonicated for further 1 h to get uniform solution, before the pH was adjusted to 8 by NH4OH. Hereafter, the blend was put in water bath at 80 °C for 4 h. The prepared sample was assembled by centrifugation and washed by d-H2O, before it was dried at 60 °C for 2 h.

2.2 *Material Characterization*

The synthesized FeOOH and FeOOH/rGO were undergone inspection of X-ray diffraction (XRD) was performed using (Shimadzu XD-1) with Cu Kα radiation (λ=0.1542 nm) at a beam voltage of 40 kV and 40 mA beam current. The data was picked up in a 2θ range of 4-80° and 0.7° s−1 scan rate at 25 °C.

Fourier transform infrared spectroscopy (FTIR) was carried out using (ATI Mattson 1001) at 400–4000 cm−1 wavenumber. The Raman spectra was carried out using the Renishaw Invia-Raman spectrometer equipped with a He Ne laser (532-nm excitation wavelength, 50-mw total power) which operated under 5% of the power with range from 100 to 3600 waves, extended scanning for 10 s and cumulative number of three times. The surface area parameters were estimated through N2 adsorption/desorption isotherms at liquid N2 (−196 °C) using (NOVA 3200 Unit, USA apparatus). High resolution transmission electron microscopy (HRTEM) was carried out by (JEOL 2100F TEM) with 200 kV accelerating voltage.

2.3 Catalytic activity

The liquid phase process properties were examined through batch model to test the desulfurization performance of FeOOH and FeOOH/rGO nanocomposites in the diesel fuel model. For all trials, an exact amount of each nanocomposite was added to 10 mL of DBT stock solutions (1000 ppm, in dodecane). Then, the removal activity was examined under the following operating conditions; the adsorbent amount (5, 10, 20 g); H2O2:S molar ratio (3:1,13:1,18:1); and the reaction time (10-120 min). The analysis included filtration of the catalyst from the mixture and the DBT concentration was measured using GC-FPD, where the following equations represent how we estimated the adsorption capacity and desulfurization rate:

$$q_t = mM \times C_0 - C_i \times 10^{-3} \quad (1)$$

$$W = C_0 - C_t / C_0 \times 100 \quad (2)$$

where *"q_i"* is the sulfur adsorption capacity of the adsorbent (mg S. mg^{-1}); "*m*" is the weight of oil model (g); *"M"* is the weight of the adsorbent (mg); *"C_0"* and *"C_i"* are the start and end sulfur proportions in the oil model, respectively; *"W"* is the equilibrium S-concentrations in the oil model.

2.4 Kinetics of the DBT removal by the synthesized FeOOH

The kinetics of DBT adsorptive removal using FeOOH were analyzed using the models reported by Ho & McKAy [11], that resulted in two model's pseudo-first order & pseudo-second order (Equations. 1, 2). The two models were employed to unravel the mechanism governing the adsorption process. The mass transfer process or chemisorption is assumed to be the rate-limiting step in these models. Additionally, the rate of adsorption estimated utilizing the following model equations:

$$\ln(q_e - q_t) = \ln(q_e) - k_1 t \quad (3)$$

$$\frac{1}{q_t} = \frac{1}{q_e^2 k_2} + \frac{1}{q_e} \quad (4)$$

where, "q_e" and q_t are the equilibrium adsorption capacity (mg/g) and at time *t* (min), respectively; "k_1" (min^{-1}) and "k_2" (g/mg. min) are the rate constants of pseudo-first order and second order, respectively.

2.5 Thermodynamics of the DBT removal by FeOOH

Activation energy can be obtained by the Arrhenius equation:

$$\ln K_2 = \ln A - \frac{E_a}{RT} \quad (5)$$

where "*A*": Arrhenius factor, "E_a": Arrhenius activation energy (kJ/mol), which obtained from the slope of ln*K* versus 1/T curve, "*R*": the gas constant (8.314 J/mol.K), and "*T*": the temperature in Kelvin (K).

3. Results and discussion

3.1 Catalyst characterization

The diffractograms of the graphite oxide (GO), FeOOH, and FeOOH/rGO are depicted in Figure (1a), where all the labeled peaks are ascribed to a tetragonal FeOOH phase (JCPDS file no. 34-1266), manifesting that the FeOOH was synthesized with no considerable impurities. Moreover, these diffraction patterns were vividly demonstrated in the FeOOH/rGO composite, indicating that the FeOOH was successfully combined with the chemically reduced GO. On the other hand, the FTIR patterns of the GO, FeOOH, and FeOOH/rGO were illustrated in Figure (1b). The intensity of the absorption peaks of the synthesized GO was evident for the corresponding structural OH group (3300 cm-1) [12], C=O groups of the carboxyl and carbonyl moieties (1627 cm-1), in addition to the carboxyl group (1396 cm^{-1}), and C-O vibration of the alkoxyl or the epoxy groups (1055 cm-1) [14]. Moreover, the hydroxyl group bands were obvious at 3345; 1620; 1390; and 1040 cm-1 for both the synthesized FeOOH and FeOOH/rGO, while the bands assigned to the vibration states of the Fe-O emerged at 856 and 667 cm^{-1} [14, 15].

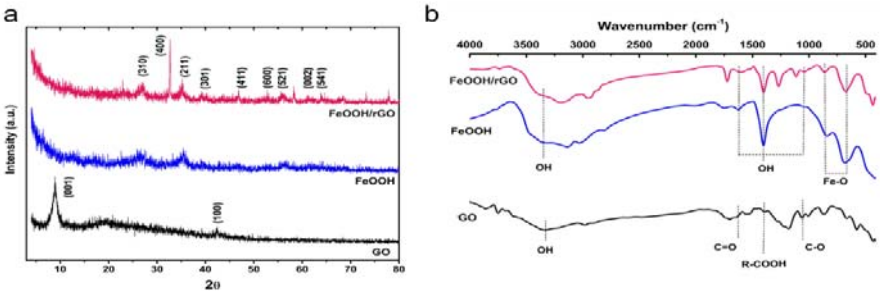

Figure 1. (a) XRD and (b) FTIR of the prepared rGO, FeOOH, and FeOOH/rGO.

The Raman spectra of GO and FeOOH/rGO nanocomposites are displayed in Figure 6. Two distinct bands are visible in both spectra. both the G and D bands. It is discovered that the ID/IG values for GO and CuO/rGO nanocomposites are, respectively, 0.81 and 1.69. The inclusion of FeOOH NPs onto GO sheets results in a reduction of GO, as seen by the slightly higher ID/IG value, slightly greater shift of the G band, and slightly lower shift of the D band in the Raman spectra of FeOOH/rGO nanocomposites [16].

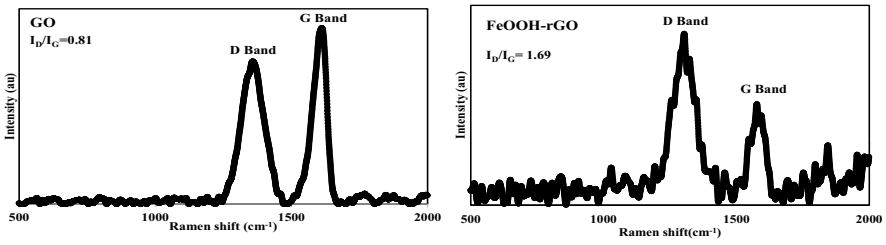

Figure 2. Raman Spectrum of GO and FeOOH/rGO nanocomposite

The N2 adsorption/desorption parameters of the FeOOH and FeOOH/rGO were depicted in Figure (3a). The results of the BET method declared that the FeOOH/rGO composite exhibit improved surface area and pore volume (219 m2/g and 0.268 cc/g, respectively). It is clearly evident that the higher specific superficial area and pore volume exhibited by the FeOOH/rGO composite are not only correlated with higher adsorption potentialities, but bestows more active sites, which contribute for catalytic activity as well.

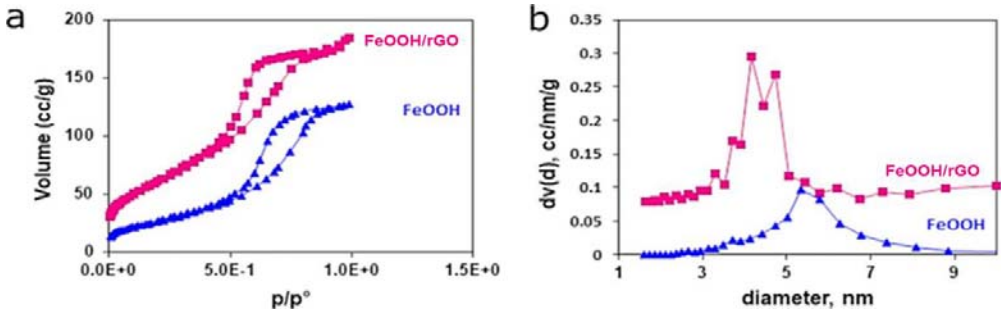

Figure 3. (a) N_2 adsorption/desorption, and (b) the pore diameter of the created FeOOH, and FeOOH/rGO.

The investigation of the nano-structure of the synthesized materials by the TEM showed the formation of the characteristic rGO sheets (Figure 4a), in addition to the FeOOH in ultrathin nanorods shape, where their mean diameter recorded about 4.52±0.9 nm, while the length average was about 28.5±9.5 nm measured by Image J® software (average of 20 nanorods) (Figure 4b & c). Wei et al. reported their synthesis for ultrathin α-FeOOH nanorods with about 25 nm diameter and 75 nm length. Furthermore, the FeOOH/rGO nanocomposite appeared integrated where the FeOOH nanorods were crowded on the surface of the graphene sheet, as another clue of the prevalence of the synthesis route [17].

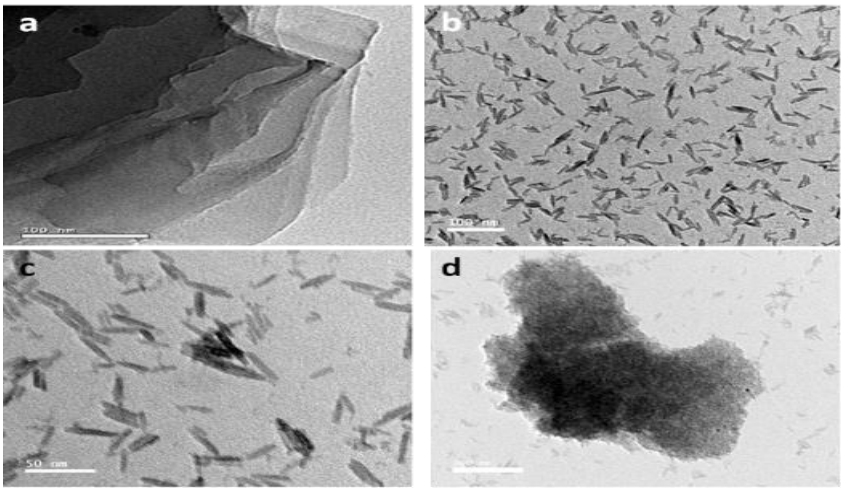

Figure 4. TEM imaging of the synthesized (a) rGO; (b &c) FeOOH; and (d)FeOOH/rGO.

3.2 Catalytic activity

First, using the prepared FeOOH, various conditions were tested for the adsorptive/oxidative desulfurization of DBT as a model diesel fuel. These conditions included adsorbent amount, reaction time period, and the presence of different H2O2:S ratios. Then, the optimum conditions were selected and applied using FeOOH/rGO system to study the role of rGO in adsorption process.

Regarding the FeOOH amount adopted for the best DBT removal, we examined the removal behavior of the FeOOH amounts: 5, 10, 15, and 20 mg at the reaction time (60 min).

As shown in Figure (5a), the DBT concentration decreased from 1000 ppm to 40 ppm (i.e ~96% removal efficiency) by utilizing 20 mg of FeOOH, while adopting only 10 mg of the adsorbent reduced the DBT

to about 60 ppm (i.e ~94% removal efficiency). So, from an economical viewpoint, the 10 mg of the catalyst was considered the optimal catalyst weight to complete the study.
However, as Figure (5b) illustrates, the removal efficiency rises as the H2O2 ratio does when a FeOOH system is present. According to this data, FeOOH can function as a powerful catalyst to improve DBT oxidation by H2O2, converting it into the form of sulfones or sulfoxides. Because of the presence of O=S=O, which is more polar than S in DBT, this system has elevated adsorptive affinity for sulfoxides and sulfones than thiophenic compounds. As a result, the in-situ absorptivity of the sulfur compounds on FeOOH system improved [18]. The ideal H2O2: S ratio of 18:1 was discovered, at such point the removal efficiency was approximately 94%, and the FeOOH needed to lower the DBT concentration from 750 to 60 ppm was evaluated.

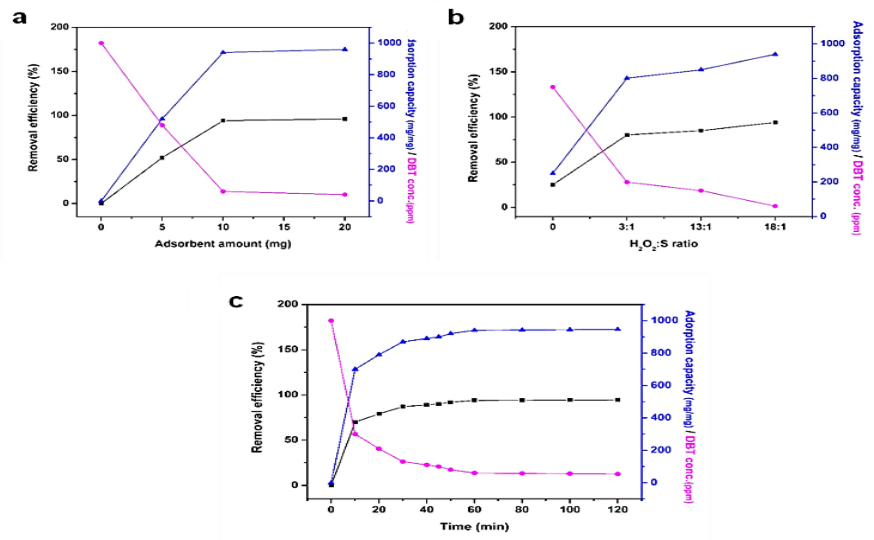

Figure 5. Influence of (a) adsorbent amount; (b) H_2O_2:S ratio; and (c) reaction time on the DBT removal by FeOOH.

Additionally, the adsorption kinetics were investigated at mild temperature using an initial DBT proportion of 1000 ppm, an adsorbent concentration of 10 g/L, and an 18:1 H2O2: S ratio to estimate the minimum equilibrium time of the removal reaction. The kinetic curves of DBT removal over FeOOH (Figure 5c) demonstrate that the DBT withdrawal rate accelerated at the initial phase, and then it turned slower near the chemical balance. This is explained by the fact that there are many empty active sites in the reaction beginning that are actively engaged in the early stages of the treatment time. Later on, however, the remaining empty surface sites become difficult to occupy due to forces that are repulsive between the solution phase and the DBT adsorbed on the FeOOH surface.
Removing 94% of the sample was found to have an equilibrium time of 60 mins. According to the theory, the FeOOH fraction readily forms the free hydroxylation surface when H+ is present, producing FeOOH that is positively charged. Therefore, an outer surface coordination complex between the sulfonic and FeOOH is achieved when the formed (FeOOH+) increases the electrostatic attraction with the negatively charged sulfonic group.
Figure (6a, b) represents the kinetic data for DBT removal using the prepared FeOOH sample. According to the higher correlation coefficient values (R2), pseudo-second order model is more typical for this process. This implies that the DBT removal reaction is more precisely described by “chemisorption”, which suggests the evolving of covalent bonds facilitates the electrons sharing between the binding sites of the FeOOH and the adsorbate.

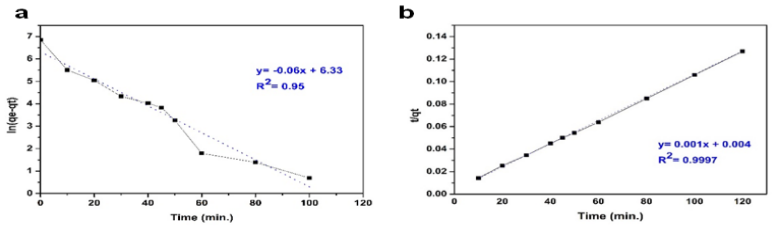

Figure 6. Reaction kinetics of the DBT removal by the synthesized FeOOH

The parameters of the thermodynamic enthalpy change (ΔH), Gibbs energy change (ΔG), and entropy change (ΔS) were detected using the following equations:

$$\Delta G = -RT \ln K \qquad (6)$$

$$\Delta G = \Delta H - T\Delta S \qquad (7)$$

where "R" is the gas constant with a value of 8.314 J $K^{-1}mol^{-1}$; "T" is the temperature in kelvin (K); "lnK" is the natural logarithm of the equilibrium constant K.

The data are illustrated in Table (1) showing that (ΔS) and (ΔH) exerted positive values indicating an endothermic catalytic oxidation/adsorption process resulting in increasing disorder. ΔG becomes more negative as temperature increases, which indicates an increase in the degree of spontaneity by increasing the temperature. The magnitude of triggering energy was also adopted to conclude the type of adsorption reaction, where the Ea showed 85.4 kJ/mol which gives unambiguous evidence that the adsorption of DBT onto FeOOH is assorted as a chemical adsorption.

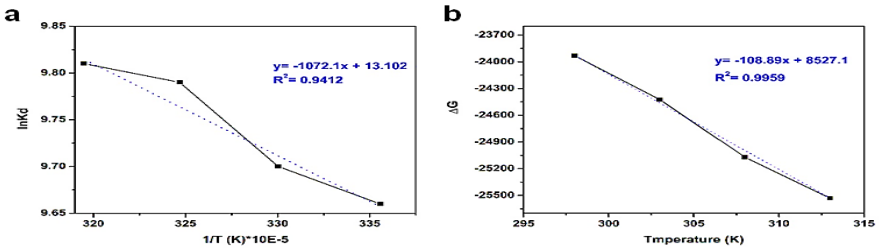

Figure 7. Reaction thermodynamics of the DBT removal by the synthesized FeOOH.

Table 1. Thermodynamic parameters of the DBT removal by the FeOOH.

T (Kelvin)	ΔG0	ΔH0	ΔS0	Ea (kJ/mol)
298	-23932	8527.1	108.89	85.4
303	-24424			
308	-25071			
313	-25531			

FeOOH/rGO exhibits the highest removal efficiency of 98.9% when 10 g/L of catalyst is used, confirming the critical role that rGO plays in FeOOH/rGO. ability to function as a catalyst for the oxidative-adsorptive desulfurization process.

4. Conclusion

We synthesized ultrathin nanorods and FeOOH/reduced graphene oxide (rGO) nanocomposite through a facile precipitation route, where their chemical and physical properties were carefully studied. The XRD, FTIR and ramen spectra have shown that the synthesis route was eminent, which was further emphasized by the TEM inspection. The BET examination indicated that the synthesized materials possess elevated active surface area.The catalytic activity of the DBT removal reaction by the FeOOH was studied, while the kinetics of the reaction accredited that the DBT removed by chemisorption reaction type through oxidative/ adsorptive desulfurization processes using H2O2 as green oxidant. The thermodynamic study demonstrated that FeOOH's desulfurization capacity increased with temperature and that FeOOH/rGO can function as an outstanding oxidant/adsorbent in the sulfur removal processes with an elimination efficiency of 98.9%. Finally, we can declare that the FeOOH/rGO nanocomposite is an incredibly promising oxidant-adsorbent for the ODS process.

Acknowledgements

A. M. M. and D. R. A. are grateful for the Egyptian Petroleum Research Institute (EPRI) for supporting this work. D. A. is thankful for The City of Scientific Research and Technological Applications (SRTA-City) supporting this work.

References

[1] Xu J, Zhang B, Lu Y, Wang L, Tao W, Teng X, Ning W and Zhang Z 2022 *J. Hazard. Mater* **421** 126680
[2] Wang T, Li X, Dai W, Fang Y and Huang H 2015 *J. Mater. Chem. A* **3** 21044
[3] Matloob A, Abd El-Hafiz D, Saad L, Mikhail S and Guirguis D 2019 *J. Hazard. Mater* **373** 447
[4] Ban L, Liu P, Ma C and Dai B 2013 *Catal. Today* **211** 78
[5] Liu Y, Zuo P, Wang R and Jiao W 2022 *Fuel* **324** 124534
[6] Abdul-Kadhim W, DeRaman M, Abdullah S, Tajuddin S, Yusoff M, Taufiq-Yap H and Rahim M 2017 *J. Environ. Chem. Eng* **5** 1645
[7] Margeta D, Sertić-Bionda K, and Foglar L 2016 *Appl Acoust* **103** 202
[8] Sachdeva T and Pant K 2010 *Fuel Process. Technol* **91** 1133
[9] García-Gutiérrez J, Fuentes G, Hernández-Terán M, García P, Murrieta-Guevara F and Jiménez-Cruz F 2008 *Appl Catal A-Gen* **334** 366
[10] Kabi T, Hildebrandt D, Liu X and Yao Y 2022 *J. Environ. Manage* **309** 114598
[11] Ho Y and McKay G 1998 *Process Saf Environ Prot* **76** 332
[12] Al-Hagar O, Abol-Fotouh D, Abdelkhalek E, Abo Elsoud M and Sidkey N 2021 *Mater. Chem. Phys* **273** 125147
[13] Arif Sher Shah M, Zhang K, Park A, Kim K, Park N, Park J and Yoo P 2013 *Nanoscale* **5** 5093
[14] Millan, A., Urtizberea, A., Natividad, E., Luis, F., Silva, N. J. O., Palacio, F., Mayoral, I., Ruiz-González, M. L., González-Calbet, J. M., Lecante, P., & Serin, V. (2009). Polymer, 50(5), 1088–1094.
[15] Shawky, S., El-Hafiz, D. R. A., Shalaby, N. H., Said, S., Helal, M. H., & Mohamed, S. K. (2022). Materials Chemistry and Physics, 278, 125625.
[16] Ajay Gupta, Raman Jamatia, Ranjit A. Patil, Yuan-Ron Ma, and Amarta Kumar PalACS Omega 2018 3 (7), 7288-7299
[17] Wei, Y., Ding, R., Zhang, C., Lv, B., Wang, Y., Chen, C., Wang, X., Xu, J., Yang, Y., & Li, Y. (2017. Journal of Colloid and Interface Science, 504, 593–602.
[18] Wang, T., Li, X., Dai, W., Fang, Y., & Huang, H. (2015). Journal of Materials Chemistry A, 3(42), 21044–21050.